ELECTRONIC SUPPLEMENTARY INFORMATION

Achieving low-carbon future through the Energy-Chemical Nexus in China

Yinan Li,[1,#] Song Lan,[1,#] Javier Pérez-Ramírez,[1,2,*] Xiaonan Wang[1,*]
[1] Department of Chemical and Biomolecular Engineering, National University of Singapore, 4 Engineering Drive, Singapore 117585, Singapore
[2] Institute for Chemical and Bioengineering, Department of Chemistry and Applied Biosciences, ETH Zurich, HCI E125, Vladimir-Prelog-Weg 1, 8093 Zurich, Switzerland
# These authors contributed equally to this work
*Correspondence: chewxia@nus.edu.sg (X.W.) jpr@chem.ethz.ch (J.P-R.)

S1. Data collection

Electricity data

The electricity data for the 2018 baseline scenario is sourced from the China Electric Power Yearbook 2018 [1]. For the future electricity data, we first collect the predicted national electricity data of 2050 from the official document, China Energy and Power Development Outlook [2], provided by State Grid Energy Research Institute of China. Then, by assuming an equal growth rate, the electricity capacity and demand for each province are predicted based on the 2018 regional electricity demand. The solar and wind power installed capacities of each province are predicted based on the assessment of China's solar and wind resources at provincial level [3,4].

Methanol data

In order to obtain the methanol data of the 2018 baseline scenario, we first collect data through public sources, such as industrial reports, published papers and public data from National Bureau of Statistics. Then, a full-sample sampling, which covers interview transcripts, surveys and monitoring data of 190 companies with methanol production qualifications in China, is conducted. For the data which cannot be obtained directly from public sources and sampling, both bottom-up and top-down calculation methods are used to reckon and verify the data based on the obtained relative information. All these obtained data were verified by cross-comparisons in order to ensure the data close to the actual situation. In China, methanol is widely employed in chemical industries, such as in the synthesis of formaldehyde, methyl tertiary butyl ether (MTBE), dimethyl ether (DME), which are important materials for the development of the modern construction, transportation, and chemical industries. For the future scenarios of methanol demand and production capacity, linear growth rates in future 30 years are predicted by most of the projections [5–8]. In this study, we use historical methanol demand and production capacity in China between 2004 and 2018 to calculate the corresponding linear growth rates, which are shown in Figure S1. Then China's regional methanol for 2050 is projected by assuming an equal growth rate for all the provinces. Considering the policy of widely promoting methanol vehicles in China [5], we assume a 2.3 times

growth rates of methanol demand for the 2050 nexus-v scenario. For the potential of shale gas development in China, the production capacity of natural gas-based methanol for 2050 nexus-s scenario is predicted based the calculated linear grow rate from 2004 and 2018. Approximately 82.6% of methanol is transported by overland freight in China [9]. In our paper we assumed that all the methanol is transported by overland freight.

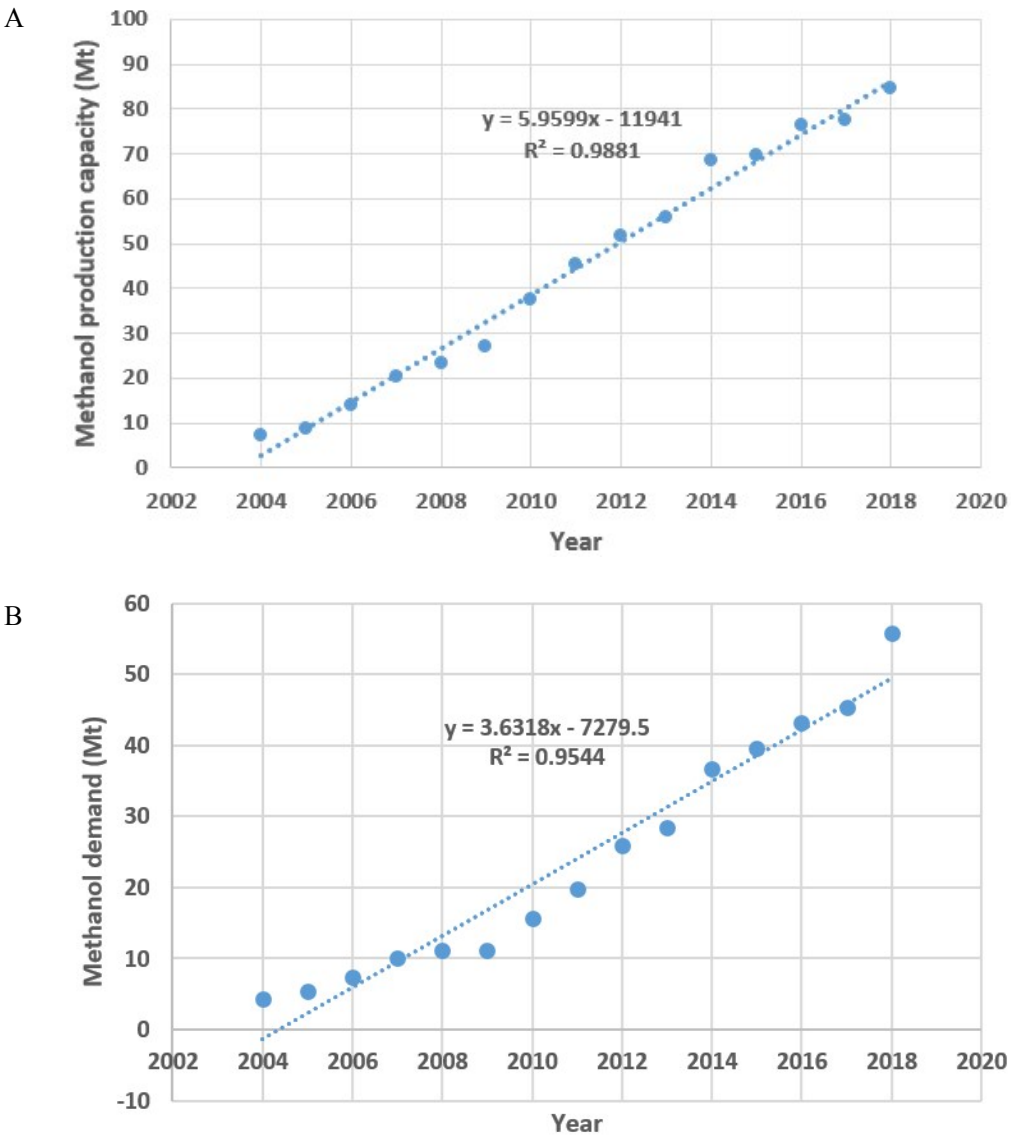

Figure S1: Historical methanol data from 2004 to 2018 and their projections into the future. *Linear growth is assumed for methanol production capacity and demand in China for the next 30 years, which is supported by both expert views and historical trends. The growth rates for capacity and demand are estimated from historical data as shown in (A) and (B), respectively.*

Technology cost data

For energy sector, the current national average levelised costs of electricity (LCOE) for coal, coal-CCS, natural gas, natural gas-CCS, nuclear, wind, solar, biomass and BECCS technologies in China are taken from a global markup study by Morris *et al.* [10] while that for hydropower is taken from International Renewable Energy Agency (IRENA) [11]. All costs are converted to 2018 RMB and

subsequently projected to 2050 based on the global trends of LCOE for each technology available at Open Energy Information (OpenEI) transparent cost database [12]. The provincial difference in LCOE in China is assumed to be constant across time and consistent with that in electricity price published in China Electric Power Yearbook 2018 [1]. For chemical sector, the current national average levelised costs for coal, coke-oven gas and natural gas-based methanol production and its road transportation in China are obtained from our own data collection as explained above. The cost for CO_2-based methanol synthesis is taken from Pérez-Fortes *et al*. [13]. Again, all costs are first converted to 2018 RMB and then projected to 2050 based on the cost breakdown for conventional and CCU plants in [13] taking into account various price indices for China from National Bureau of Statistics [14]. The levelised cost of hydrogen from electrolysis excluding cost of electricity is calculated from a recent report of International Energy Agency (IEA) [15], which is converted to 2018 RMB and projected to 2050 based on predictions in the same report. Due to the unavailability of relevant data at province-level resolution, the costs of methanol and hydrogen are assumed to be constant across all provinces.

Technology emissions data

For energy sector, the cradle-to-gate life cycle inventories (LCI) for coal, natural gas, nuclear, hydro, wind and solar-based power generation in China are taken from ecoinvent database v3.5 [16] with province-level resolution. For natural gas-CCS, the LCIs of a natural gas combined cycle (NGCC) power plant in Beijing, China are first retrieved from ecoinvent database as reference, with the effects of CCS facilities subsequently evaluated based on Singh *et al.* [17]. The LCIs for coal-CCS, biomass and BECCS technologies are taken from Yang *et al.* [18] with China related assumptions. The LCIs for coal-CCS, natural gas-CCS, biomass and BECCS are assumed to be constant across all provinces. For chemical sector, the LCIs for coal and coke-oven gas-based methanol production in China are taken from Li *et al.* [19] while those for natural gas-based production and road transportation are retrieved from ecoinvent database. The comprehensive LCIs for hydrogen production from water electrolysis including both construction and operation phases are adopted from Icelandic New Energy [20]. The LCIs for all methanol production routes, road transportation and water electrolysis are assumed to be constant across all provinces.

S2. Planetary boundaries life cycle assessment (PB-LCA)

The general workflow for incorporating the emerging concept of planetary boundaries (PB) into conventional life cycle assessment (LCA) in order to form a new framework (PB-LCA) for absolute sustainability analysis is outlined in Figure S2.

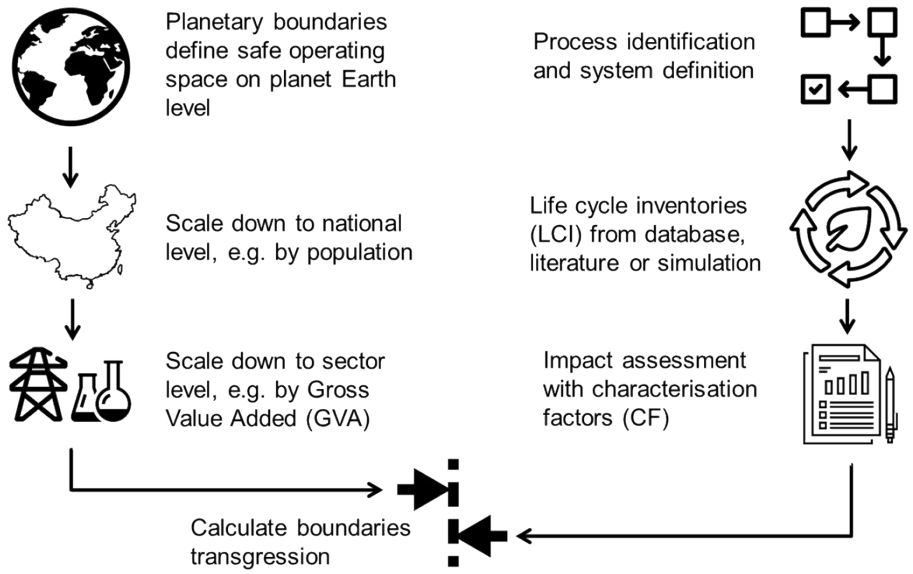

Figure S2: General workflow for planetary boundaries life cycle assessment.
Planetary boundaries initially define safe operating spaces on planet Earth level, thus are downscaled proportionally first to national level by population and subsequently to sectors level by gross value added. The life cycle inventories of processes under study can be obtained from a variety of sources including database and literature, and then multiplied by characterisation factors to get the impact scores on planetary boundaries. Comparing impact scores and safe operating spaces, boundaries transgression can be calculated.

As shown by Figure S2, the PB-LCA framework can be roughly divided into two phases, i.e. the downscaling phase (left branch) and the characterisation phase (right branch), before boundaries transgression can be calculated. For the downscaling phase, population and gross value added (GVA) have been selected as the two criteria for global-to-national and national-to-sectorial boundaries downscaling, respectively in this work. Denote safe operating space of boundary k at planet level as b_k^{global},

$$b_k^{national} = \frac{POP^{China}}{POP^{world}} \cdot b_k^{global} \#(\text{Equation S1})$$

where $b_k^{national}$ is the safe operating space of boundary k at national level, POP^{China} and POP^{world} are China and world populations, respectively. Further downscaling to the energy-chemical nexus level,

$$b^{nexus}_{k} = \frac{GVA^{electricity} + GVA^{methanol}}{GDP^{China}} \cdot b^{national}_{k} \#(\text{Equation S2})$$

where b^{nexus}_{k} is the safe operating space of boundary k at nexus level, GDP^{China} is the gross domestic product (GDP) of China, $GVA^{electricity}$ and $GVA^{methanol}$ are the GVA of electricity and methanol sectors, respectively. It is to be noted that since cradle-to-gate LCIs are used to calculate impact scores in this work, the GVA of relevant upstream economic activities are lumped into the GVA of selected sectors under analysis, whose reason can be explained as follows. Take the simple supply chain, *coal mining → coal-fired power generation*, as an illustrative example, emissions from both activities are accounted in cradle-to-gate LCIs of power generation, but the former activity adds value to mining sector while the latter adds value to electricity sector. Thus, in order to match GVA with LCIs, the GVA of those mining activities that are upstream of power generation is added to the GVA of power sector.

Due to data unavailability and lack of clear definition of some boundaries, the following eight boundaries are selected for consideration in this work with their downscaled safe operating spaces shown in Table S1. The safe operating spaces at planet Earth level refer to the differences between planetary boundaries [21] and their natural background levels [22]. The population data for China and the world are obtained from World Bank [23]. The total GVA for electricity and methanol sectors are calculated from China's input-output tables published by National Bureau of Statistics [24].

Table S1: Safe operating spaces of selected planetary boundaries.

Planetary boundary	Unit	Safe operating space (global)	Safe operating space (selected sectors of China)
Climate change (energy imbalance at top of atmosphere)	W/m^2	1	0.005
Climate change (atmospheric CO_2 concentration)	ppm CO_2	72	0.329
Stratospheric ozone depletion	DU	15	0.069
Ocean acidification	Ω_{arag}	0.69	0.003
Biogeochemical flows (nitrogen, global)	Tg N/year	62	0.283
Biogeochemical flows (phosphorus, global)	Tg P/year	9.9	0.045
Land-system change (global)	%	25	0.114
Freshwater use (global)	km^3/year	4000	18.277

For characterisation phase, the impact scores of relevant processes on those previously selected PBs are calculated as the following.

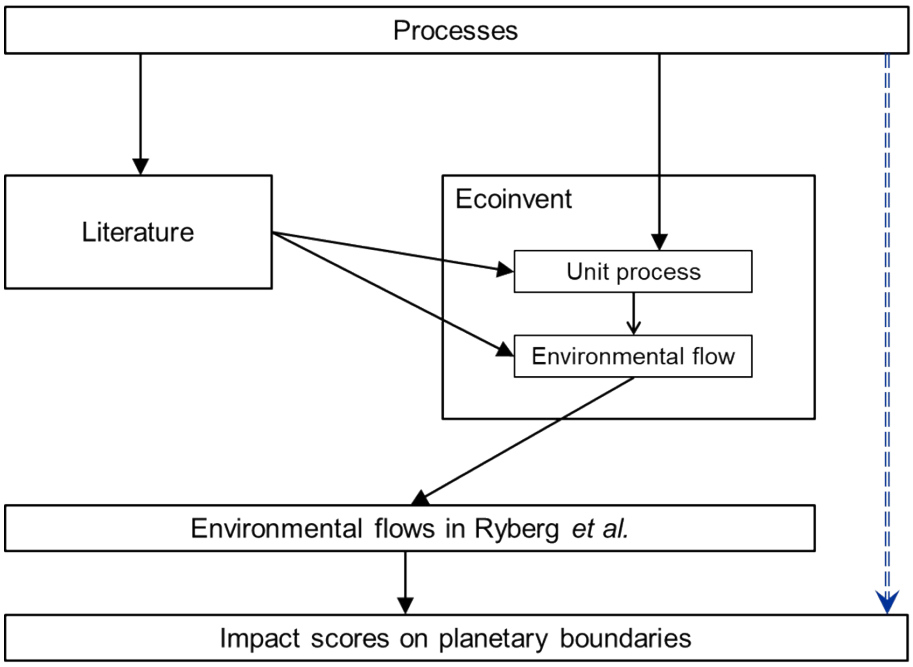

Figure S3: Workflow for process impact assessment.

A direct mapping from processes to impact scores on planetary boundaries (thick dashed blue arrow) can be established with ecoinvent database as an intermediate. Technologically mature processes can be readily found in ecoinvent database. For emerging technologies, their life cycle inventories are obtained from literatures whose processes and environmental flows can be mapped to ecoinvent counterparts as well. Within the database, cumulative life cycle inventories for unit processes are provided, thus eventually life cycle inventories for all processes in our work can be expressed by the set of over 2000 environmental flows in ecoinvent database. Characterisation factors for various planetary boundaries can be obtained from Ryberg et al. [25] *whose environmental flows are also mapped to those in ecoinvent database.*

For process i in province j considered in this work, denote its life cycle inventory for environmental flow l as $LCI_{i,j,l}$. Then its impact score on planetary boundary k, denoted by $IM_{i,j,k}$, can be calculated as

$$IM_{i,j,k} = \sum_{l} f_{k,l} \cdot LCI_{i,j,l} \#(\text{Equation S3})$$

where $f_{k,l}$ is the characterisation factor of boundary k for environmental flow l. Summing over all processes in all provinces, for boundary k its transgression, denoted g_k, is defined as

$$g_k = \begin{cases} 0 & if \sum_{i,j} IM_{i,j,k} < b_k \\ \sum_{i,j} IM_{i,j,k} - b_k & otherwise \end{cases} \#(\text{Equation S4})$$

where b_k is the safe operating space of planetary boundary k. For the analysis of energy-chemical

nexus in this work, it equals b_k^{nexus} as calculated previously. As an emerging field still undergoing active research, planetary boundaries analysis is a rather stringent framework for sustainability assessment and quantifies the rigorous safe operating space for human activities. It is not very likely that all boundaries can be respected. Thus, define total boundaries transgression as

$$\sum_k \frac{1}{b_k} \cdot g_k \# \text{(Equation S5)}$$

which serves as a single-valued indicator for environmental impact assessment.

S3. Nexus optimisation

The nexus optimisation model developed in this work can either minimise total boundaries transgression,

$$\min \sum_k \frac{1}{b_k} \cdot g_k \#(\text{Equation S6})$$

where b_k and g_k are the safe operating space and transgression of boundary k, respectively, or minimise total cost,

$$\min \sum_{i,j} c_{i,j} x_{i,j} + \sum_{i,i'} \alpha d_{i,i'} p_{i,i'} \#(\text{Equation S7})$$

where $c_{i,j}$ and $x_{i,j}$ are the cost and usage of technology j in province i, respectively. α is the cost of methanol transportation per distance in unit of [money·mass^{-1}·distance^{-1}]. $d_{i,i'}$ measures the distance between province i and i' while $p_{i,i'}$ represents the amount of methanol transported from province i to i'.

Both optimisation objectives are subject to the following constraints. Firstly, both electricity and methanol demands must be satisfied at all provinces, thus

$$\sum_j s_{i,j}^E x_{i,j} - \sum_{i'} m_{i,i'} + \sum_{i'} \left(1 - \eta d_{i',i}\right) m_{i',i} \geq r_i^E \quad \forall i \#(\text{Equation S8})$$

where $s_{i,j}^E$ is the electricity supplied by unit adoption of technology j in province i and it assumes a negative value if electricity is consumed by the technology. $m_{i,i'}$ represents the amount of electricity transmitted from province i to i' while η measures the transmission loss rate in unit of [%·distance^{-1}]. In this work, a loss rate of 0.62% per 100 km is assumed according to Galán-Martín *et al.* [26]. r_i^E is the electricity demand of province i. And

$$\sum_j s_{i,j}^M x_{i,j} - \sum_{i'} p_{i,i'} + \sum_{i'} p_{i',i} \geq r_i^M \quad \forall i \#(\text{Equation S9})$$

where $s_{i,j}^M$ is the methanol supplied by unit adoption of technology j in province i and r_i^M is the

methanol demand of province i. Also, from mass balance, the consumption of captured CO_2 and hydrogen must be supplied by relevant technologies, thus

$$\sum_j s_{i,j}^C x_{i,j} \geq 0 \quad \forall i\# \text{(Equation S10)}$$

and

$$\sum_j s_{i,j}^H x_{i,j} \geq 0 \quad \forall i\# \text{(Equation S11)}$$

where $s_{i,j}^C$ and $s_{i,j}^H$ are the carbon captured and hydrogen supplied by unit adoption of technology j in province i, respectively. Their values will be negative for consumption. Due to the intermittent natural of hydro, wind and solar power, their generation needs to be backed up before grid integration by conventional controllable thermal generation technologies, i.e. coal, coal-CCS, natural gas, natural gas-CCS, biomass and BECCS. However, if that intermittent electricity is consumed on the spot by water electrolysis to produce methanol from captured CO_2, no back-up is required. Thus,

$$\varepsilon\left(\sum_{j \in I} s_{i,j}^E x_{i,j} + \sum_{j \in G} s_{i,j}^E x_{i,j}\right) \leq \sum_{j \in T} s_{i,j}^E x_{i,j} \quad \forall i\# \text{(Equation S12)}$$

where technology sets I = {hydro, wind, solar power}, G = {electrolysis, CO_2 hydrogenation} and T = {coal, coal-CCS, natural gas, natural gas-CCS, biomass, BECCS power}. ε is the electricity back-up rate for intermittent resources, which is taken to be 20% in this work according to Galán-Martín *et al.* [26]. The adoption of all technologies should be within their respective capacities and all decision variables are required to be non-negative. Thus,

$$x_{i,j} \leq u_{i,j} \quad \forall i,j\# \text{(Equation S13)}$$

where $u_{i,j}$ represents the capacity of technology j in province i and

$$x_{i,j}, m_{i,i'}, p_{i,i'}, g_k \geq 0 \quad \forall i,i',j,k\# \text{(Equation S14)}$$

Finally, in order to measure boundary transgression,

$$\sum_l f_{k,l}\left(\sum_{i,j} e_{i,j,l} x_{i,j} + \sum_{i,i'} t_{i,i',l} d_{i,i'} p_{i,i'}\right) \leq b_k + g_k \quad \forall k\# \text{(Equation S15)}$$

where $f_{k,l}$ is the characterisation factor of boundary k for environmental flow l. $e_{i,j,l}$ measures the

emission of environmental flow l by technology j in province i while $t_{i,i',l}$ is the emission of environmental flow l by methanol transportation from province i to i' per distance in unit of [mass·mass^{-1}·distance^{-1}]. For cost optimisation, total boundaries transgression can serve as an additional constraint,

$$\sum_k \frac{1}{b_k} \cdot g_k \leq \lambda \#(\text{Equation S16})$$

where λ is the allowance for total transgression. After optimisation, the cost of solution can be calculated as

$$\sum_{i,j} c_{i,j} x_{i,j} + \sum_{i,i'} \alpha d_{i,i'} p_{i,i'} \#(\text{Equation S17})$$

while total boundaries transgression can be calculated as

$$\sum_k \frac{1}{b_k} \cdot \max\left(\sum_l f_{k,l}\left(\sum_{i,j} e_{i,j,l} x_{i,j} + \sum_{i,i'} t_{i,i',l} d_{i,i'} p_{i,i'}\right) - b_k, 0\right) \#(\text{Equation S18})$$

S4. Curtailment calculation

The curtailment rate of renewable energy (hydro, wind and solar) can be calculated as follow,

$$C = \frac{P_{cap,r} - P_{gen,r}}{P_{cap,r}} \times 100\% \#(\text{Equation S19})$$

where C and $P_{gen,r}$ are the curtailment of renewable energy and generated electricity from renewable energy, respectively. $P_{cap,r}$ is maximum power capacity of renewable energy, which is calculated based on the installed capacity of renewable energy.

$$P_{cap} = G_{ins} \times 24 \times 365 \times CF \#(\text{Equation S20})$$

G_{ins} is the installed capacity of renewable energy. CF is the capacity factor, which is estimated from the electricity data of 2018. $P_{gen,r}$ requires an additional 20% grey electricity to back-up the intermittent electricity for grid connection. Thus,

$$20\% \cdot P_{gen,r} + P_{gen,g} \leq P_{cap,g} \#(\text{Equation S21})$$

where $P_{cap,g}$ and $P_{gen,g}$ are respectively the maximum power capacity of grey energy and generated electricity from grey energy.

S5. Interactive visualisation

There are 31 provinces excluding Hong Kong, Macau and Taiwan in China that are considered in this work and the nexus optimisation model involves 10 technologies of electricity generation, 4 technologies of methanol production and one technology of hydrogen production for each province. Also, inter-provincial transmission of electricity and transportation of methanol are allowed in the optimisation model. Thus, there could be $31 \times (10 + 4 + 1) + 31 \times 31 + 31 \times 31 = 2387$ decision variables in total, emphasising the importance of good visualisation tools for results analysis. In this work, the optimisation model is solved by SciPy linear programming solvers [27] whose results are directly written to json files with Python. With the help of Echarts libraries [28], the results can be readily visualised interactively with JavaScript. The complete interactive visualisation codes are available on GitHub at https://github.com/Yinan-LI/GEP-visualization.git. Please refer to the provided link for visualisations with full functionality and high resolution while the following figures are only snapshots for a brief illustration on its usage.

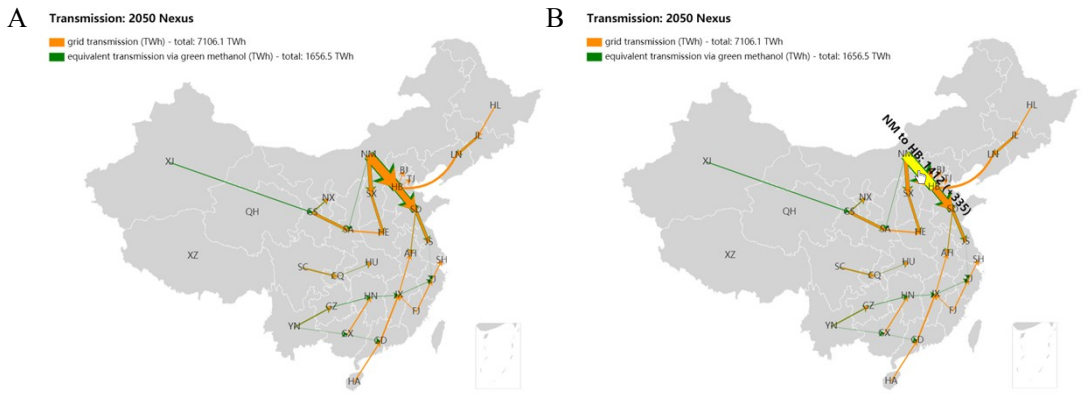

Figure S4: Electricity and green methanol transmission plot for 2050 nexus scenario.
Scenario name, legend and corresponding key statistics, i.e. total transmission amount via grid and green methanol, are shown on the top left corner of figure, as in (A). When mouse pointer hovers over an arrow, the source, destination as well as exact amount of electricity and green methanol transmission represented by that arrow are shown above the arrow. The number in plain text and that in parenthesis with plus sign in front represent electricity and methanol, respectively, as in (B). Similar plots for other scenarios (not shown here) are also generated.

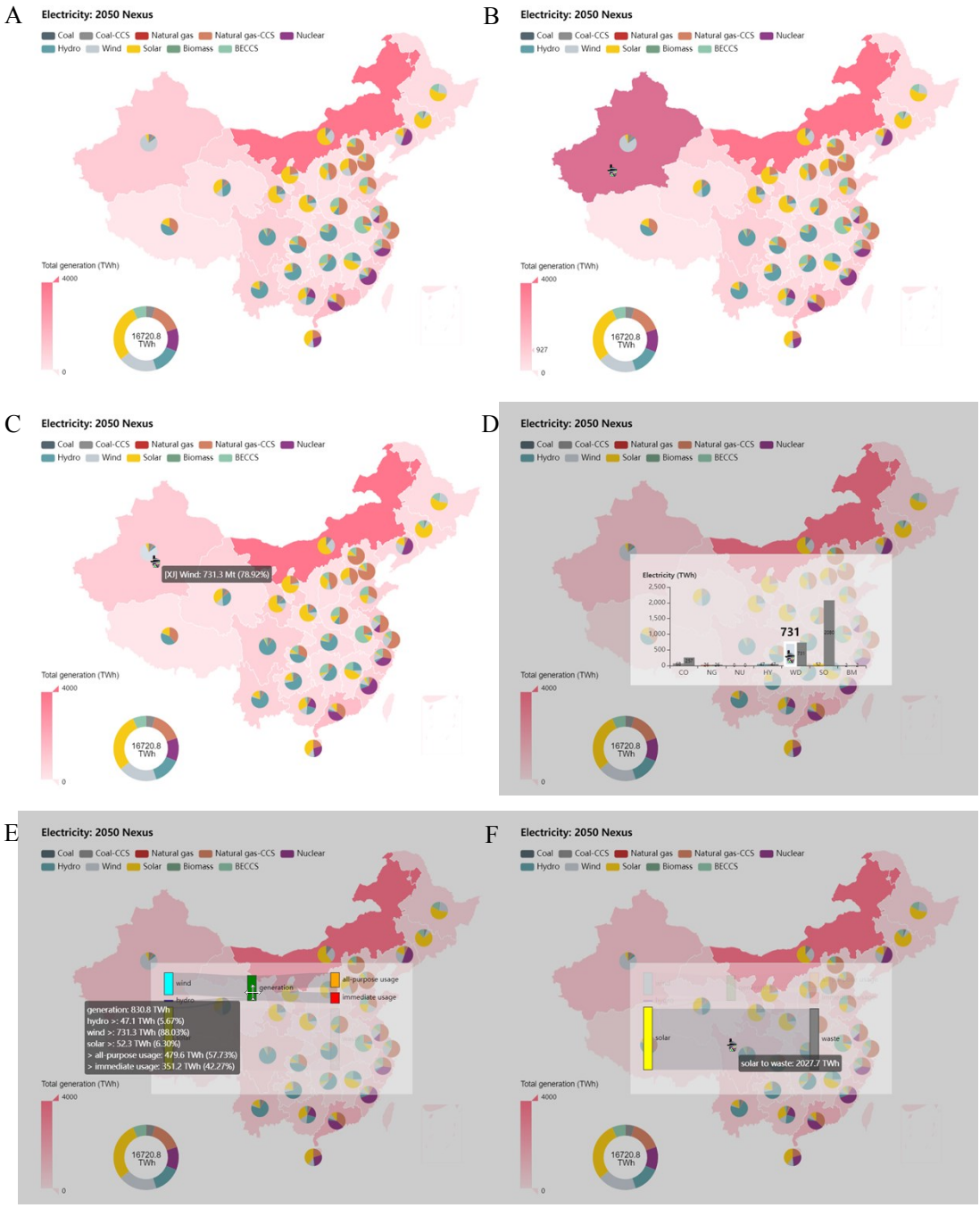

Figure S5: Electricity generation technologies plot for 2050 nexus scenario.

Scenario name and legend are shown on the top left corner of figure while the national technology mix and total amount of electricity generation are shown on the bottom left corner, as in (A). When mouse pointer hovers over a province, its background is highlighted with provincial generation amount shown on the color bar at the bottom left corner of figure, as in (B). When mouse pointer hovers over a slice of the pie chart on a province, abbreviated province name, technology name, generation amount of that technology and its percentage for that province are shown in the tooltip, as in (C). When any pie chart or province background is clicked, a bar chart showing generation amount (left colored bar) and capacities (right gray bar) of each technology for that province is popped up. When mouse pointer hovers over any bar, the exact number of that bar is shown with its border highlighted in white, as in (D). When any bar is clicked, a Sankey chart showing the flow of

intermittent renewable resources (hydro, wind and solar) is popped up. When mouse pointer hovers over any node, the exact value of that node, as well as the inflows to that node with percentage (denoted by node name followed by a ">" sign) and the outflows from that node with percentage (denoted by a ">" sign followed by node name), is shown in the tooltip, as in (E). When mouse pointer hovers over any edge, the exact value of that flow is shown in the tooltip, as in (F). When the gray background of (D), (E) or (F) is clicked, the bar or Sankey chart is cleared and the figure is reverted back to (A). Also, mouse drag and zoom are enabled in (A) for the convenience of visualisation, and when mouse pointer hovers over or clicks on the doughnut chart for national technology mix, similar effects to those for provincial pie charts are presented. Similar plots for other scenarios (not shown here) are also generated.

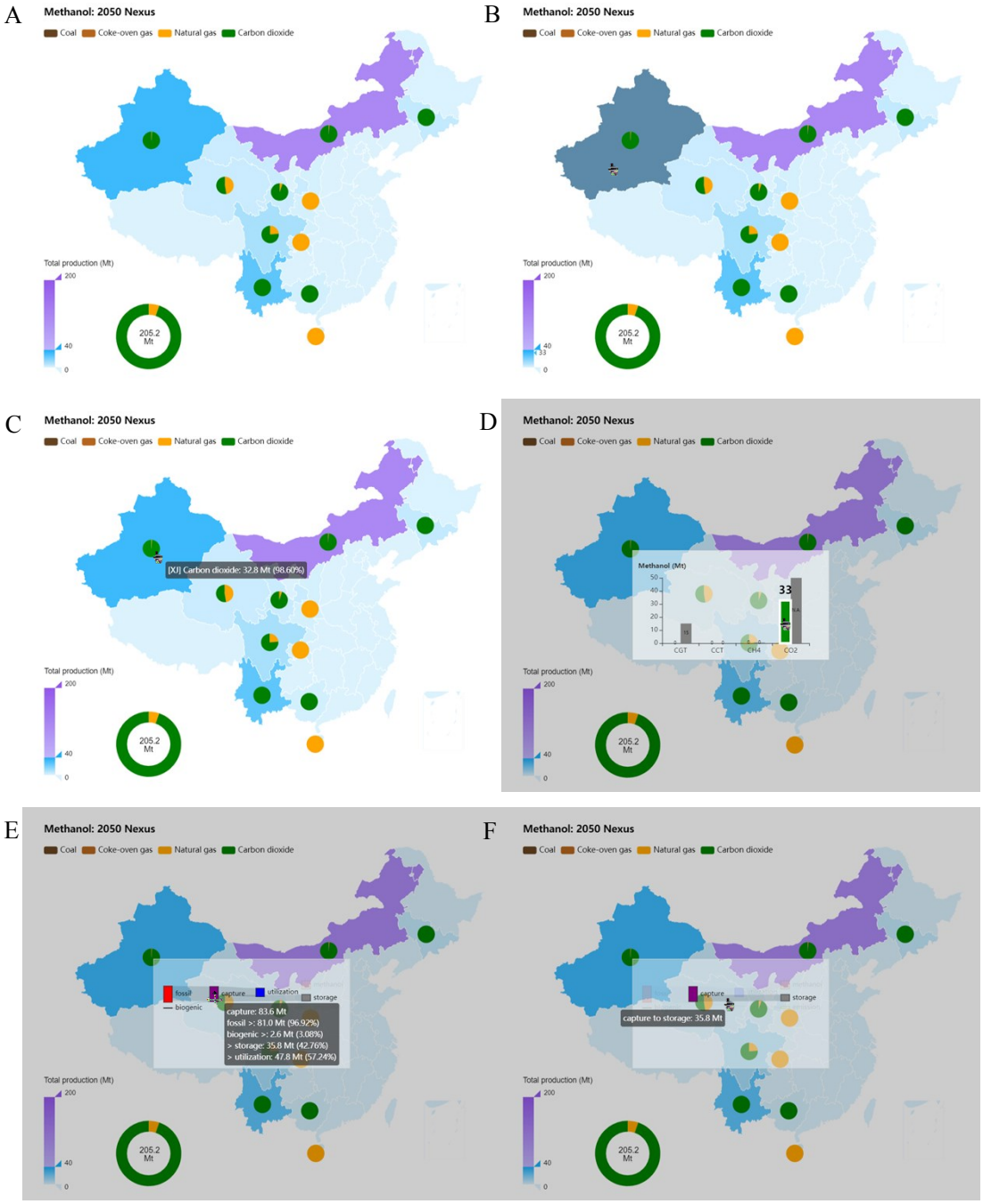

Figure S6: Methanol production technologies plot for 2050 nexus scenario.

Scenario name and legend are shown on the top left corner of figure while the national technology mix and total amount of methanol production are shown on the bottom left corner, as in (A). Regarding the map's color encoding, due to the vast difference in amount of methanol produced by each province, blue is used to represent production amount less than 40 Mt/year while purple is used to represent that above 40 Mt/year, as reflected in the color bar. When mouse pointer hovers over a province, its background is highlighted with provincial production amount shown on the color bar at the bottom left corner of figure, as in (B). When mouse pointer hovers over a slice of the pie chart on a province, abbreviated province name, technology name, production amount of that technology and its percentage for that province are shown in the tooltip, as in (C). When any pie chart or province background is clicked, a bar chart showing production amount (left colored

bar) and capacities (right gray bar) of each technology for that province is popped up. Note that due to the very high capacities of CO_2-based production, they are not fully shown in the bar charts for most provinces. However, the exact number of any bar, including the one for CO_2-based production, is always shown with its border highlighted in white when mouse pointer hovers over that bar, as in (D). When any bar is clicked, a Sankey chart showing the flow of carbon dioxides is popped up. When mouse pointer hovers over any node, the exact value of that node, as well as the inflows to that node with percentage (denoted by node name followed by a ">" sign) and the outflows from that node with percentage (denoted by a ">" sign followed by node name), is shown in the tooltip, as in (E). When mouse pointer hovers over any edge, the exact value of that flow is shown in the tooltip, as in (F). When the gray background of (D), (E) or (F) is clicked, the bar or Sankey chart is cleared and the figure is reverted back to (A). Also, mouse drag and zoom are enabled in (A) for the convenience of visualisation, and when mouse pointer hovers over or clicks on the doughnut chart for national technology mix, similar effects to those for provincial pie charts are presented. Similar plots for other scenarios (not shown here) are also generated.

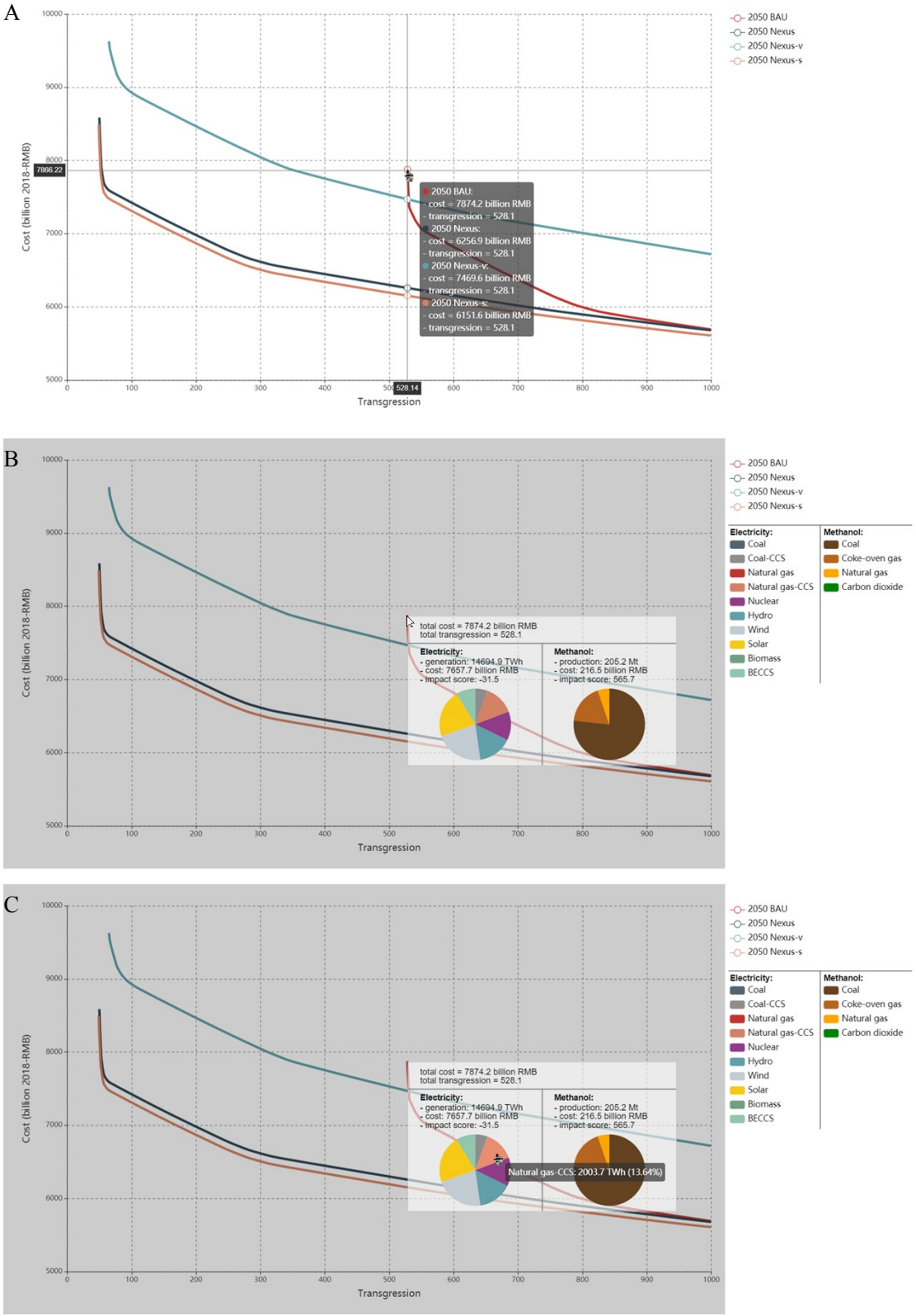

Figure S7: Pareto fronts of nexus optimisation.

The optimal trade-off curves between total cost and total boundaries transgression are shown for the four 2050 scenarios with legends on the top right corner of figure. All cost components are projected to 2050 and expressed in 2018-RMB as explained in Section S1. When mouse pointer hovers over the curves, scenario names together with their corresponding costs and boundaries

transgression are shown in the tooltip for all four scenarios at the same value of total transgression, as in (A). When a point on any curve is clicked, several key statistics associated with that point including production quantities, costs and impact scores for both electricity and methanol sectors are shown. Two pie charts showing national technology mixes for both sectors are also popped up with legends shown in the right unshaded region of figure, as in (B). When mouse pointer hovers over a slice of any pie chart, technology name, production quantity of that technology and its percentage are shown in the tooltip, as in (C). When the gray background of (B) or (C) is clicked, the pie charts and their legends are cleared, and the figure is reverted back to (A). Also, mouse drag and zoom are enabled in (A) for the convenience of visualisation.

S6. The Chinese context

The assessment from geographical, energy sectoral, chemical sectoral, economic and environmental perspectives in the main text all leads to a common conclusion that CO_2-based methanol production is beneficial to China. However, it does not necessarily imply that CO_2-to-methanol is a universally superior alternative worldwide, especially for those countries with abundant natural gas resources. Table S2 compares the carbon footprints of methanol production from various conventional methods as well as the four future scenarios for 2050 considered in this work.

Table S2: Comparison between carbon footprints of various methanol production routes.

Methanol production route	Carbon footprint (kg $CO_{2\text{-eq}}$/kg methanol)	Source
Coal-based	17.7	[19]
Scenario: 2050 BAU	14.1	Calculation
Coke-oven gas-based	2.89	[19]
Scenario: 2050 nexus-v	0.951	Calculation
Scenario: 2050 nexus-s	0.859	Calculation
Scenario: 2050 nexus	0.856	Calculation
Natural gas-based	0.617	[16]

As can be seen from Table S2, the carbon footprint of natural gas-based methanol production is considerably lighter than those for coal and coke-oven gas-based production. For CO_2-based methanol production, its carbon footprint heavily depends on the source of electricity. According to [13], 0.199 kg H_2 is typically required per kg methanol produced while water electrolysis consumes 53 kWh electricity [20] per kg H_2 produced. Therefore, in order to make the carbon footprint of CO_2-to-methanol smaller than that of natural gas-based process, the maximum carbon footprint of electricity generation is 0.0585 kg $CO_{2\text{-eq}}$/kWh. Among the three major renewable resources, only wind and hydro power can meet such requirement. The overall carbon footprints of 2050 nexus scenarios are around 0.86 kg $CO_{2\text{-eq}}$/kg methanol and 0.95 kg $CO_{2\text{-eq}}$/kg methanol under the assumptions of linear and super-linear growth for methanol demand, respectively. Those values are still higher than that of natural gas-based production but substantially smaller than coal and coke-oven gas-based methods. Consider the facts that natural gas is not a widely abundant resource in China and the government has decided not to further expand natural gas-based methanol production capacity since 2012 [29], CO_2-based methanol production does have advantages in the achievement of low carbon future in China, although it may not be the best solution worldwide.

Also, it is interesting to note that despite the higher natural gas-based methanol production capacity in 2050 nexus-s scenario, its carbon footprint of methanol production is slightly higher than that of 2050 nexus scenario. This can be explained by the "burden shifting" effect commonly seen in nexus analysis, i.e. the expenditure incurred in one partition results in larger savings of the rest, thus benefiting the entire system, with the help of interactive visualisation tools introduced in previous section. Hydropower, as a very clean source of renewable energy, is mainly distributed in Southwest China, e.g. Sichuan and Yunnan provinces, as shown in Figure 3 of main text. Take Yunnan province as an example, from Figure S8, it can be seen that the capacities of hydropower in Yunnan

province have been exhausted for electricity generation in both scenarios, however, more electricity and thus hydropower is consumed for water electrolysis in 2050 nexus scenario as compared to 2050 nexus-s scenario.

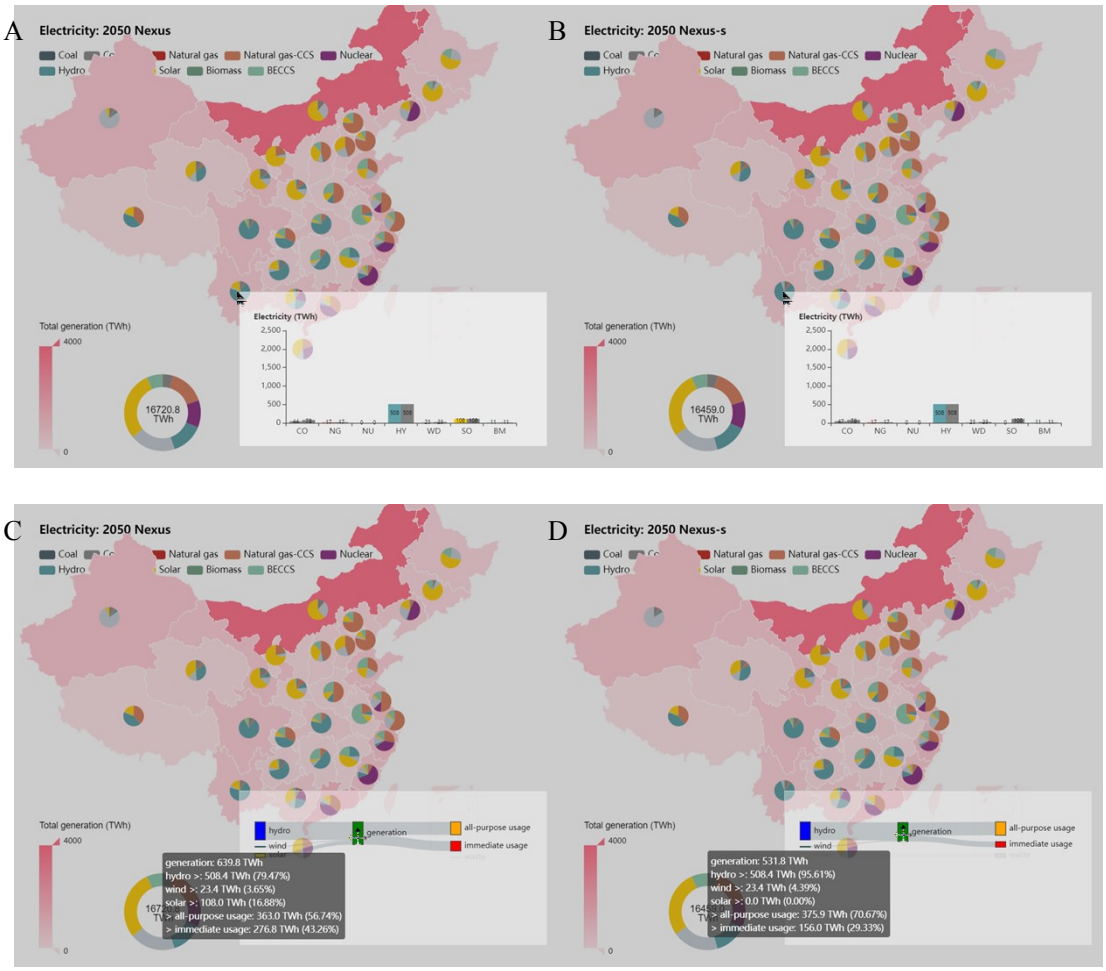

Figure S8: Electricity generation of Yunnan province for 2050 nexus and 2050 nexus-s scenarios.

From (A) and (B), the capacities of hydropower in Yunnan province have been fully exploited in both scenarios. However, in 2050 nexus scenario (C), 276.8 TWh of renewable energy is used locally for water electrolysis, among which hydropower constitutes 276.8 × 79.47% = 220.0 TWh according to the provincial generation mix. For 2050 nexus-s scenario (D), due to the increase in natural gas-based methanol production capacity in China, less hydrogen is required for CO_2-based production and only 156.0 × 95.61% = 149.2 TWh of hydropower is consumed locally for water electrolysis according to the renewable generation mix in Yunnan province.

Due to the very light carbon footprint of hydropower, this makes the overall carbon footprint of electricity for hydrogen production via electrolysis smaller in 2050 nexus scenario as compared to 2050 nexus-s scenario. Since the carbon footprint of CO_2-to-methanol heavily depends on its source of hydrogen, the carbon footprint of methanol production in 2050 nexus scenario is correspondingly lower. On the other hand, the increment in natural gas-based production capacity for 2050 nexus-s scenario partially substitutes CO_2-based methanol production in 2050 nexus scenario, thus releasing

some hydropower from electrolysis to fulfill social electricity demand and decarbonise the power sector. Therefore, although the carbon footprint of methanol production is slightly higher in 2050 nexus-s scenario as compared to 2050 nexus scenario, the overall environmental impact of the former is lower than that of the latter, as seen from Figure 9 of main text.

Nomenclature:

For Section S2:

Symbol	Definition
b_k^{global}	safe operating space of planetary boundary k at planet Earth level
$b_k^{national}$	safe operating space of boundary k at national level
b_k^{nexus}	safe operating space of boundary k at energy-chemical nexus level
POP^{world}	world population
POP^{China}	population of China
GDP^{China}	GDP of China
$GVA^{electricity}$	total GVA of electricity sector including relevant upstream activities
$GVA^{methanol}$	total GVA of methanol sector including relevant upstream activities
$IM_{i,j,k}$	impact score on planetary boundary k for process i in province j
$LCI_{i,j,l}$	life cycle inventory of environmental flow l for process i in province j
$f_{k,l}$	characterisation factor of boundary k for environmental flow l
b_k	safe operating space of boundary k
g_k	transgression of boundary k

For Section S3:

Symbol	Definition
Indices	
i	provinces (alias i')
j	technologies
k	planetary boundaries
l	environmental flows
Sets	
I	{hydro, wind, solar power}
G	{electrolysis, CO_2 hydrogenation}
T	{coal, coal-CCS, natural gas, natural gas-CCS, biomass, BECCS power}
Parameters	
$d_{i,i'}$	distance between province i and i'
r_i^E	electricity required by province i
$s_{i,j}^E$	electricity supplied by technology j in province i, negative value for consumption
ε	electricity back-up rate for intermittent resources
η	electricity transmission loss rate

r_i^M	methanol required by province i
$s_{i,j}^M$	methanol supplied by technology j in province i, negative value for consumption
$s_{i,j}^C$	carbon captured by technology j in province i, negative value for consumption
$s_{i,j}^H$	hydrogen supplied by technology j in province i, negative value for consumption
$u_{i,j}$	capacity of technology j in province i
$c_{i,j}$	cost of technology j in province i
α	cost of methanol transportation per distance
$e_{i,j,l}$	emissions of environmental flow l by technology j in province i
$t_{i,i',l}$	emissions of environmental flow l by methanol transportation from province i to i' per distance
$f_{k,l}$	characterisation factor of boundary k for environmental flow l
b_k	safe operating space of boundary k
λ	allowance for total transgression
Decision variables	
$x_{i,j}$	use of technology j in province i
$m_{i,i'}$	electricity transmission from province i to i'
$p_{i,i'}$	methanol transportation from province i to i'
g_k	transgression of boundary k

For Section S4:

Symbol	Definition
C	curtailment of renewable energy
G_{ins}	installed capacity of renewable energy
CF	capacity factor of renewable energy
$P_{cap,\,r}$	maximum power capacity of renewable energy
$P_{cap,\,g}$	maximum power capacity of grey energy
$P_{gen,\,r}$	generated electricity from renewable energy
$P_{gen,\,g}$	generated electricity from grey energy

References:

1 CEPY, *China Electric Power Yearbook*, China Electric Power Press, Beijing, 2018.

2 State Grid, China Energy and Power Development Outlook, http://www.sohu.com/a/280406624_662580, (accessed 19 February 2020).

3 G. He and D. M. Kammen, *Renew. Energy*, 2016, **85**, 74–82.

4 G. He and D. M. Kammen, *Energy Policy*, 2014, **74**, 116–122.

5 C. Li, M. Negnevitsky and X. Wang, in *Energy Procedia*, Elsevier Ltd, 2019, vol. 160, pp. 324–331.

6 Q. Chen, Y. Gu, Z. Tang and Y. Sun, *Energy Convers. Manag.*, 2019, **187**, 63–75.

7 M. Alvarado, *IHS Chem. Bull. 3*, 2016, 10–11.

8 Argus, *Argus Global Methanol Annual 2018*, 2018.

9 L. W. Su, X. R. Li and Z. Y. Sun, *Energy Policy*, 2013, **63**, 130–138.

10 J. Morris, J. Farrell, H. Kheshgi, H. Thomann, H. Chen, S. Paltsev and H. Herzog, *Int. J. Greenh. Gas Control*, 2019, **87**, 170–187.

11 IRENA, *Renewable Power Generation Costs in 2018*, International Renewable Energy Agency, Abu Dhabi, 2019.

12 Open Energy Information, Transparent Cost Database, https://openei.org/wiki/Transparent_Cost_Database, (accessed 28 May 2020).

13 M. Pérez-Fortes, J. C. Schöneberger, A. Boulamanti and E. Tzimas, *Appl. Energy*, 2016, **161**, 718–732.

14 National Bureau of Statistics, National Data, http://data.stats.gov.cn/easyquery.htm?cn=A01&zb=A010101&sj=202004, (accessed 28 May 2020).

15 IEA, *The Future of Hydrogen*, Paris, 2019.

16 ecoinvent, ecoinvent Version 3.5 Database, https://v35.ecoquery.ecoinvent.org/Search/Index, (accessed 10 February 2020).

17 B. Singh, A. H. Strømman and E. Hertwich, *Int. J. Greenh. Gas Control*, 2011, **5**, 457–466.

18 B. Yang, Y. M. Wei, Y. Hou, H. Li and P. Wang, *Appl. Energy*, 2019, **252**, 113483.

19 C. Li, H. Bai, Y. Lu, J. Bian, Y. Dong and H. Xu, *J. Clean. Prod.*, 2018, **188**, 1004–1017.

20 Icelandic New Energy, *Generation of the energy carrier hydrogen – in context with electricity buffering generation through fuel cells*, 2008.

21 W. Steffen, K. Richardson, J. Rockstrom, S. E. Cornell, I. Fetzer, E. M. Bennett, R. Biggs, S. R. Carpenter, W. de Vries, C. A. de Wit, C. Folke, D. Gerten, J. Heinke, G. M. Mace, L. M. Persson, V. Ramanathan, B. Reyers and S. Sorlin, *Science (80-.).*, 2015, **347**, 1259855–1259855.

22 M. W. Ryberg, M. Owsianiak, J. Clavreul, C. Mueller, S. Sim, H. King and M. Z. Hauschild, *Sci. Total Environ.*, 2018, **634**, 1406–1416.

23 World Bank, Population, total - China, https://data.worldbank.org/indicator/SP.POP.TOTL?locations=CN&view=chart, (accessed 13 February 2020).

24 National Bureau of statistics of China, Input-Output Tables of China, http://data.stats.gov.cn/ifnormal.htm?u=/files/html/quickSearch/trcc/trcc01.html&h=740, (accessed 10 February 2020).

25 M. W. Ryberg, M. Owsianiak, K. Richardson and M. Z. Hauschild, *Ecol. Indic.*, 2018, **88**, 250–262.

26 A. Galán-Martín, C. Pozo, A. Azapagic, I. E. Grossmann, N. Mac Dowell and G. Guillén-Gosálbez, *Energy Environ. Sci.*, 2018, **11**, 572–581.

27 Optimization and Root Finding (scipy.optimize) — SciPy v1.4.1 Reference Guide, https://docs.scipy.org/doc/scipy/reference/optimize.html, (accessed 27 February 2020).

28 Apache ECharts (incubating), https://echarts.apache.org/en/index.html, (accessed 27 February 2020).

29 National Development and Reform Commission, China to ban new natural gas-based methanol plants, http://www.chemchina.com.cn/portal/xwymt/hyxw/webinfo/2012/11/1352683957825442.htm, (accessed 19 February 2020).